CODEN: WJAPAC Impact Factor: 5.48 ISSN: 3049-3013

World Journal of Advance Pharmaceutical Sciences

Volume 3, Issue 4, Page: 1-14 Research Article www.wjaps.com

VALIDATION OF A MULTICOLOR FLOW CYTOMETRY SYSTEM COMBINING AUTOMATED SAMPLE PREPARATION AND ADVANCED ANALYSIS FOR LYMPHOCYTE IMMUNOPHENOTYPING AND LYMPHOID MALIGNANCY DIAGNOSIS

Ghazala Nathu, MD[1]*; Zahid Nazir, MD[1]; Adila Nathu, MD[1]; Cyril Erica, MLS(ASCP)CM[1], Irfan Khan, PhD[2], Muhammad Ashir MBBS, MS[2]

[1]ADSCIS Laboratory, Waterford, New York 12188, United States.
[2]University at Albany, Department of Chemistry, Albany, New York 12222, United States.

How to cite this Article: Ghazala Nathu, MD[1]*; Zahid Nazir, MD[1]; Adila Nathu, MD[1]; Cyril Erica, MLS(ASCP)CM[1], Irfan Khan, PhD[2], Muhammad Ashir MBBS, MS[2] (2026). VALIDATION OF A MULTICOLOR FLOW CYTOMETRY SYSTEM COMBINING AUTOMATED SAMPLE PREPARATION AND ADVANCED ANALYSIS FOR LYMPHOCYTE IMMUNOPHENOTYPING AND LYMPHOID MALIGNANCY DIAGNOSIS. World Journal of Advance Pharmaceutical Sciences, 3(4), 1-14.

Article Info

Article Received: 13 February 2026,

Article Revised: 03 March 2026,

Article Accepted: 23 March 2026.

DOI: https://doi.org/10.5281/zenodo.19307481

***Corresponding author:**

Dr. Ghazala Nathu

ADSCIS Laboratory, Waterford, New York 12188, United States.

ABSTRACT

Background: Flow cytometry has become a standard diagnostic technology in clinical hematology and immunology. The CLSI H62 guideline provides a validation framework for flow cytometric assays. Standardization and quality control remain persistent challenges, with significant inter-laboratory variability documented across platforms, reagents, and operator practices (Dorn-Beineke & Sack, 2016; Kelleher et al., 2024). **Objective:** This study validates an 8-color immunophenotyping panel for lymphoid malignancy diagnosis and a 6-color TBNK lymphocyte subset panel on the Sysmex XF-1600 platform with PS-10 automated sample preparation and VenturiOne® analysis software. The XF-1600 has demonstrated reliable performance in B-CLL diagnosis with inter-laboratory harmonization (Weir et al., 2025) and measurable residual disease assessment in multiple myeloma (Salvia et al., 2024). **Methods:** PMT voltage optimization was performed across seven fluorescence channels using Spherotech COMPtrol beads. Accuracy was assessed by method comparison of 16 specimens against a reference laboratory (Pearson correlation, Bland-Altman analysis). Precision was evaluated per CLSI EP15-A3 (5 replicates/run, 2 runs/day, 5 days). Specimen stability was tested at 0, 4, 8, 24, 48, and 72 hours. Carryover was assessed using sequential high/low acquisitions. A 25-specimen stability study across three batches with T0/T1 paired testing confirmed batch-to-batch consistency. **Results:** Optimal PMT voltages were established for all channels (peak stain indices 13.1 to 142.6). Method comparison showed Pearson $r > 0.97$ for CD3+, CD4+, and CD8+ with mean biases below 1.0 percentage point. Precision CVs were below 3.5% for major populations at normal levels. All parameters remained stable within 5% of baseline through 72 hours. Carryover was below 0.5%. **Conclusions:** The Sysmex XF-1600 with integrated automated preparation and VenturiOne® analysis meets all validation requirements for clinical lymphocyte immunophenotyping and lymphoid malignancy diagnosis.

KEYWORDS: Flow cytometry; Immunophenotyping; CLSI H62; Assay validation; Lymphoid neoplasms; PMT optimization; Sysmex XF-1600; TBNK; Standardization; Quality control.

1. INTRODUCTION

Flow cytometric analysis plays a central role in hematologic diagnostics. Clinicians rely on the technology for rapid assessment of lymphoid cell populations with abnormal phenotypes. Its primary clinical value lies in distinguishing benign reactive expansions from clonal lymphoid neoplasms and in supporting accurate disease classification (Kroft et al., 2021). Achieving diagnostic precision requires thorough immunophenotypic profiling, careful antibody selection, and standardized data interpretation (Böttcher et al., 2022).

Achieving diagnostic precision requires thorough immunophenotypic profiling, careful antibody selection, and standardized data interpretation (Böttcher et al., 2022). Panels include markers for cell lineage determination (CD19, CD3, CD5), maturation and differentiation (CD10, CD20, CD34, CD38), clonality assessment via kappa and lambda light chain expression, and disease-related abnormalities (CD23, CD200, CD103, CD56, CD117) (Hallek, 2025). Cytoplasmic markers such as cyCD3, cyCD79a, and TdT support analysis of immature or diagnostically complex cases (Gökbuget et al., 2024).

Quality assurance in flow cytometry requires attention to pre-analytical, analytical, and post-analytical variables. Dorn-Beineke and Sack (2016) documented that each step of the analytical process includes factors affecting measurement precision and accuracy, from anticoagulant selection and sample transport through staining, compensation, and data analysis. Standardization efforts from the EuroFlow consortium have demonstrated that reproducible measurements are achievable when instruments, antibody panels, and protocols are harmonized (Kalina et al., 2012). The European flow cytometry quality assurance guidelines from Kelleher et al. (2024) emphasize that laboratories should validate stability of samples, participate in external quality assessment schemes, and report results using clinically relevant units with age-matched reference ranges.

The regulatory environment for flow cytometry assays continues to evolve. Albany (2024) described the increasing scrutiny from both American and European regulatory agencies on flow cytometry- based approaches in cell therapy, emphasizing the need for quality by design principles from assay conception. The FDA January 2024 guidance on CAR-T cell products now requires documentation of assay controls, instrument calibration, QC activities, and gating strategy in initial IND submissions. For clinical diagnostic laboratories, CLSI H62 (2021) provides the validation framework for flow cytometric assays, and NYSDOH Wadsworth Center CLEP requirements define expectations for laboratory- developed tests.

The Sysmex XF-1600 flow cytometer offers a CE-IVD certified platform with three excitation lasers (blue 488nm, red 638nm, violet 405nm) and up to 10-color detection. Recent multi-center studies have validated its performance. Weir et al. (2025) demonstrated that cloned XF-1600 instrument settings eliminated inter-laboratory variability in B-CLL diagnosis across two international laboratories, with the harmonized approach matching or outperforming established Beckman Coulter Navios and BD FACSLyric systems. Salvia et al. (2024) validated the XF-1600 for MRD assessment in multiple myeloma, achieving Pearson correlation coefficients of 0.9973 to 0.9994 compared to DxFLEX and Navios EX platforms.

In this study, we report the validation of the Sysmex XF-1600 with PS-10 Sample Preparation System and VenturiOne® Analysis Software for lymphocyte immunophenotyping and lymphoid malignancy diagnosis at ADSCIS Laboratory. The validation addressed PMT voltage optimization, accuracy, precision, specimen stability, carryover, and clinical concordance.

2. MATERIALS AND METHODS

2.1 Instrumentation

All experiments were performed on the Sysmex XF-1600 Automated Flow Cytometer (Serial Number A1116) equipped with three excitation lasers: blue (488 nm), red (638 nm), and violet (405 nm).

Automated sample preparation used the Sysmex PS-10 system. Data analysis was performed using VenturiOne® Flow Cytometry Analysis Software, which provides AutoGating with contour/elliptical region positioning, automatic compensation, and statistical reporting. Data files were exported in FCS 3.0 format. A total of 69 FCS files were generated across all validation studies (Table S1, Supplementary).

2.2 Panel Configurations

Two validated panels were employed. The 8-color lymphoid malignancy panel and the 6-color TBNK lymphocyte subset panel are detailed in Tables 1 and 2.

Table 1: Lymphoid Malignancy Panel Configuration (8-Color)

Channel	Fluorochrome	B Cell	T Cell	Myeloid-1	Myeloid-2	Plasma Cell
FL1	FITC	CD5	CD2	CD11b	CD38	CD138
FL2	PE	Lambda	CD56	CD33	CD33	cyLambda
FL4	PerCP-Cy5.5	CD20	CD4	CD34	CD34	CD20
FL5	PE-Cy7	CD200	CD3	CD14	CD13	CD38
FL6	APC	CD19	CD7	CD7	CD19	CD19
FL8	APC-Cy7	CD10	CD8	CD64	CD117	CD117

FL9	Pacific Blue	Kappa	CD5	CD16	HLA-DR	cyKappa
FL10	Pacific Orange	CD45	CD45	CD45	CD45	CD45

Table 2: TBNK Lymphocyte Subset Panel Configuration (6-Color)

Marker	Fluorochrome	Clone	Target Population	Channel	Optimal Voltage
CD45	Pacific Orange	J.33	Pan-leukocyte	FL10	650V
CD3	PE-Cy7	UCHT1	T cells	FL5	Per IQ
CD4	Pacific Blue	13B8.2	Helper T cells	FL9	700V
CD8	FITC	B9.11	Cytotoxic T cells	FL1	750V
CD19	APC	J3-119	B cells	FL6	700V
CD16/56	PE	3G8/N901	NK cells	FL2	600V

2.3 Specimen Type and Processing

All specimens were EDTA-anticoagulated peripheral whole blood (100 µL per test). Specimens were processed within 24 hours of collection. Erythrocyte lysis used an ammonium chloride-based method that preserves leukocyte viability and epitope structures. A minimum of 5,000 lymphocyte-gated events were acquired per specimen.

2.4 Gating Strategy

The gating hierarchy followed CLSI H62 recommendations: (A) FSC vs SSC singlet discrimination, (B) CD45 vs SSC lymphocyte gating, (C) CD3 vs SSC for T-cell identification, (D) CD4 vs CD8 among CD3+ cells for helper and cytotoxic T-cell enumeration, (E) CD19 vs CD16/56 among CD3- negative cells for B cell and NK cell identification, and (F) CD3 vs CD19 confirmation plot. VenturiOne® AutoGating applied contour-based region positioning with region tracking across all specimens.

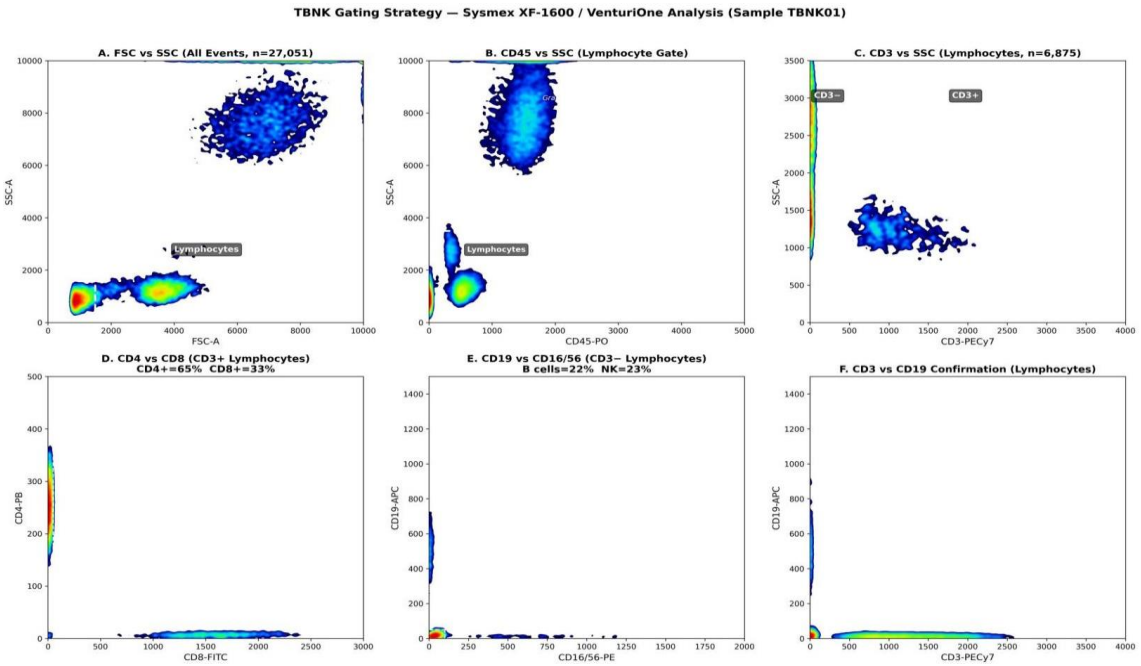

Figure 1: Representative TBNK gating strategy on the Sysmex XF-1600, analyzed with VenturiOne® software. (A) FSC vs SSC singlet discrimination. (B) CD45 vs SSC lymphocyte gate. (C) CD3 vs SSC T-cell identification. (D) CD4 vs CD8 subset discrimination. (E) CD19 vs CD16/56 B/NK identification. (F) CD3 vs CD19 confirmation. Density color: blue=sparse, red=dense events.

2.5 PMT Voltage Optimization

PMT voltage optimization followed the Sysmex XF-1600 PMT Optimization Workbook protocol using Spherotech COMPtrol antibody capture beads (CMgP-30-2K). For each fluorescence channel, two drops each of blank beads and high-affinity beads were combined with 10 µL of the corresponding fluorochrome-conjugated antibody. After 15-minute incubation in the dark at room temperature and two PBS washes, aliquots were distributed to daughter tubes. Each daughter tube was acquired at a different PMT voltage across a defined voltage series (50V increments). The stain index (SI) was calculated as (MFI positive – MFI negative) / (2 × SD negative). The voltage yielding the highest SI was

selected as optimal.

2.6 Accuracy / Method Comparison

Sixteen patient specimens spanning the clinically relevant range were analyzed in parallel on the Sysmex XF-1600 (test method) and an established reference laboratory flow cytometry method (comparator). Specimens were selected to include normal, high, and low values for CD3+, CD4+, and CD8+ percentages per CLSI H62. Statistical analysis included Pearson correlation coefficient, linear regression (slope, intercept), and Bland-Altman bias analysis with 95% limits of agreement.

2.7 Precision

Precision was evaluated per CLSI EP15-A3 and CLSI H62. Two levels of patient specimens (Normal and Abnormal/Low CD4) were tested in 5 replicates per run, 2 runs per day, over 5 consecutive days (total: 50 measurements per level per analyte). Within-run, between-run, between-day, and total precision were calculated. Acceptance criteria: CV < 5% for major populations and SD < 1.0% at low concentrations.

2.8 Specimen Stability

Single-specimen stability was evaluated at 0, 4, 8, 24, 48, and 72 hours post-collection at room temperature (18–25 °C). Percentage change from baseline (T=0) was calculated for each analyte at each time point. Acceptance criterion: < 5% change from baseline through the stated stability window. A separate 25-specimen paired stability study (T0/T1) across three batches assessed batch-to-batch consistency and confirmed the stability window under refrigerated storage (2–8 °C).

2.9 Carryover Assessment

Carryover was assessed by running a high-positive specimen (CD3+ > 80%) followed by three sequential acquisitions of a low-level specimen. Percentage recovery of the low-level specimen was calculated at each sequential position. Acceptance: carryover < 1.0% for all parameters.

3. RESULTS

3.1 PMT Voltage Optimization

PMT optimization was completed for seven fluorescence channels on the Sysmex XF-1600 (S/N A1116). Table 3 summarizes the optimal voltage and peak stain index for each channel. All channels demonstrated clear stain index peaks with defined voltage-dependent curves, confirming appropriate resolution between positive and negative bead populations.

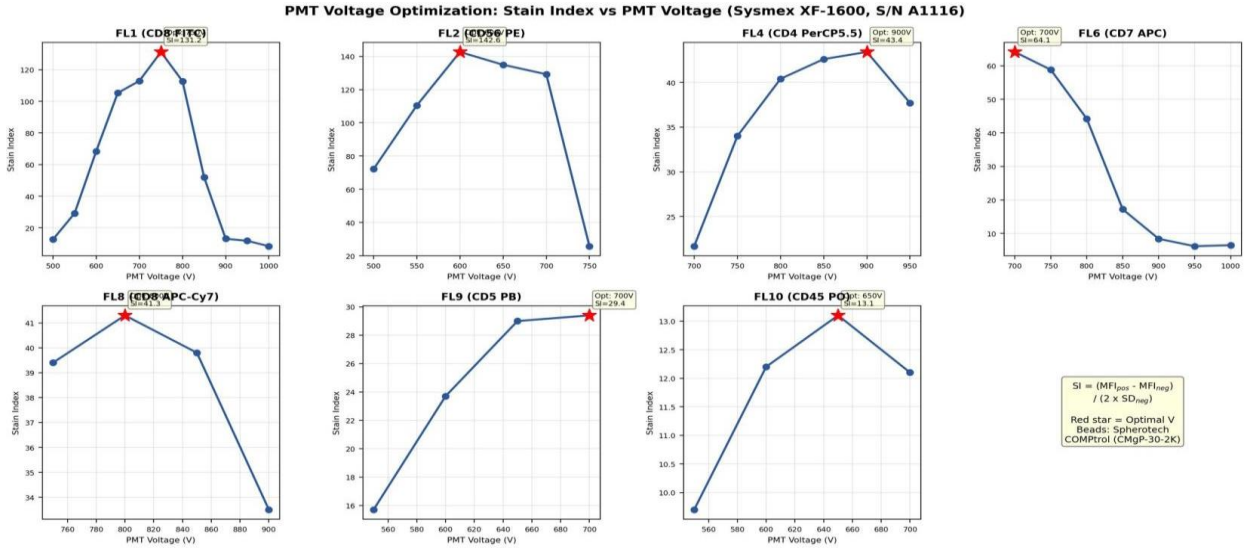

Figure 2: PMT voltage optimization curves for seven fluorescence channels. Red star indicates optimal voltage with peak stain index. Data acquired using Spherotech COMPtrol beads on Sysmex XF-1600 (S/N A1116).

Table 3: PMT Optimization Results Summary (n=7 channels)

Channel	Fluorochrome	Antibody	Voltage Range	Optimal Voltage	Peak SI	Date
FL1	FITC	CD8	500-1000V	750V	131.2	2025-11-20
FL2	PE	CD56	500-750V	600V	142.6	2025-11-20
FL4	PerCP-Cy5.5	CD4	700-950V	900V	43.4	2025-12-03
FL6	APC	CD7	700-1000V	700V	64.1	2025-12-06
FL8	APC-Cy7	CD8	750-900V	800V	41.3	2025-12-08
FL9	Blue	CD5	550-700V	700V	29.4	2025-12-08
FL10	Orange	CD45	550-700V	650V	13.1	2025-12-08

SI = Stain Index = (MFIpos – MFIneg) / (2 × SDneg). Higher SI values indicate better signal resolution.

FL2 (CD56 PE) achieved the highest peak stain index (142.6 at 600V), consistent with the bright fluorescence intensity of PE-conjugated antibodies. FL10 (CD45 Pacific Orange) showed the lowest peak SI (13.1 at 650V), reflecting the relatively lower brightness of the Pacific Orange fluorochrome.

FL1 (CD8 FITC) demonstrated a well-defined bell-shaped optimization curve across the full 500– 1000V range, with a clear peak at 750V (SI = 131.2) and a steep decline above 800V due to increasing negative-population background noise. FL6 (CD7 APC) showed the sharpest voltage sensitivity, with SI dropping from 64.1 at 700V to 6.2 at 950V.

Table 4: Detailed FL1 (CD8 FITC) PMT Optimization Data.

Tube	PMT Voltage	Pos MFI	Pos SD	Neg MFI	Neg SD	Stain Index
1	500V	34.4	3.5	0.7	1.3	12.7
2	550V	81.7	8.2	1.1	1.4	29.2
3	600V	176.8	15.3	1.8	1.3	68.4
4	650V	357.2	27.6	3.6	1.7	105.3
5	700V	687.5	56.6	7.8	3.0	112.9
6	750V	1243.0	118.4	12.1	4.7	131.2
7	800V	2178.0	191.1	24.6	9.6	112.7
8	850V	3710.0	269.4	80.2	34.9	52.0
9	900V	6376.3	522.1	487.8	224.6	13.1
10	950V	9853.4	416.6	936.5	376.8	11.8
11	1000V	9999.7	63.5	1252.1	520.4	8.4

MFI = Median Fluorescence Intensity; SD = Standard Deviation of fluorescence signal. Data from Spherotech COMPtrol beads acquired on Sysmex XF-1600, November 20, 2025.

3.2 Accuracy / Method Comparison

Sixteen patient specimens were tested on both the Sysmex XF-1600 and an established reference laboratory method. All analytes demonstrated Pearson correlation coefficients exceeding 0.97. CD4+% and CD8+ % achieved r > 0.99, indicating excellent agreement with the reference method. Mean bias for all analytes was less than 1.0 percentage point. Table 5 presents the correlation statistics. An additional 21 specimens were tested for accuracy verification of the full TBNK panel on the XF-1600, with results covering the full clinically relevant range.

Table 5: Method Comparison Correlation Statistics (n=16)

Analyte	Pearsonr	Slope	Intercept	Mean Bias (%)	95% LOA
CD3+ %	0.972	0.894	7.20	-0.30	-8.40 to 7.80
CD4+ %	0.994	1.012	0.12	0.74	-3.83 to 5.31
CD8+ %	0.994	1.034	-0.46	0.87	-3.88 to 5.62

LOA = Limits of Agreement. Acceptance criteria per CLSI H62: r ≥ 0.95, slope 0.85–1.15, mean bias < 5 percentage points. All analytes met criteria.

Figure 3 displays the distribution of each lymphocyte subset across the 21 TBNK accuracy verification specimens as box plots with overlaid individual data points. CD3+ T cells showed the tightest interquartile range (IQR), clustering between approximately 41% and 55% with a median near 48%.

This narrow spread confirms that the assay performs consistently for the predominant lymphocyte population. CD4+ helper T cells showed broader dispersion (IQR approximately 15–30%), reflecting the intentional selection of specimens with a wide range of CD4 values from low (4.9%) to high (52.4%). CD8+ cytotoxic T cells exhibited a similar spread, with outliers at the extremes (1.4% and 38.2%) that test the assay's ability to quantify both depleted and expanded populations. CD19+ B cells showed the widest relative variability, with several specimens above 30% (consistent with lymphoproliferative processes) and others below 5%. NK cells had the narrowest absolute range (1.7– 16.8%) with a median near 5.5%, concentrated in the lower portion of the scale. The inclusion of specimens with markedly abnormal distributions at both ends of the measurement range verifies that the XF-1600 performs accurately across the full clinical spectrum, not only at normal values.

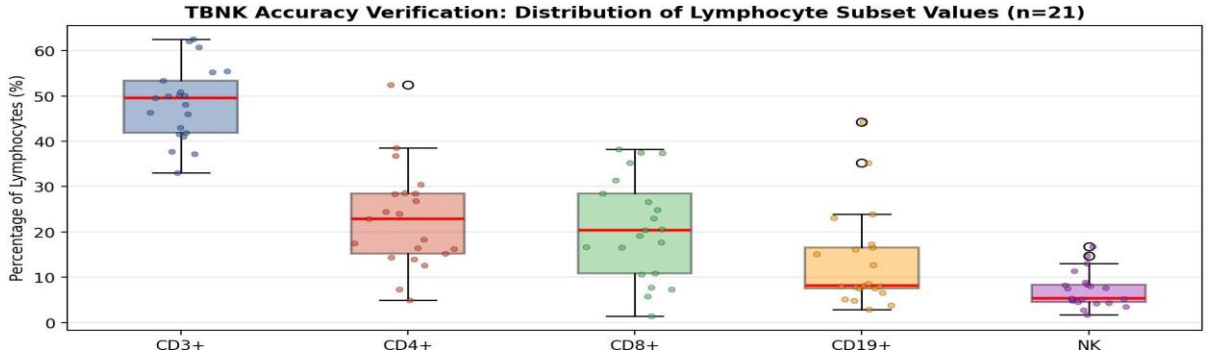

Figure 3: Distribution of lymphocyte subset values across 21 TBNK accuracy verification specimens. Box plots show median, IQR, and individual data points. CD3+ range: 33.0-62.5%, CD4+: 4.9-52.4%, CD8+: 1.4-38.2%, CD19+: 2.9-44.3%, NK: 1.7-16.8%.

Figure 4 presents Bland-Altman agreement plots for CD3+, CD4+, and CD8+ percentages, comparing the XF-1600 test method against the reference laboratory. In each panel the y-axis shows the difference between methods (XF-1600 minus Reference) and the x-axis shows the mean of both methods, allowing assessment of systematic bias and proportional error across the measurement range. For CD3+ T cells, the mean bias (red line) sits at –0.30%, indicating near-zero systematic offset between platforms. The 95% limits of agreement (orange dashed lines) span –8.40 to +7.80%, with data points distributed symmetrically above and below the bias line. No trend is visible from left to right, confirming the absence of proportional bias across low and high CD3+ values. For CD4+ helper T cells, the mean bias is +0.74% with narrower limits of agreement (–3.83 to +5.31%). The data points cluster tightly around the zero line with no fan-shaped spread at higher concentrations. This pattern indicates that the XF-1600 and reference method agree equally well whether CD4+ values are low (near 5%) or high (near 50%). For CD8+ cytotoxic T cells, the mean bias is +0.87% with limits of agreement from –3.88 to +5.62%. The scatter pattern is comparable to CD4+, with no outliers falling outside the limits of agreement. Across all three analytes, the biases are well within the CLSI H62 acceptance criterion of less than 5 percentage points, and no specimen produced a difference large enough to change clinical interpretation. The absence of proportional bias is clinically significant because it means the XF-1600 does not systematically overestimate or underestimate results at the low end of the range (where immunodeficiency decisions are made) or at the high end (where lymphocytosis is evaluated).

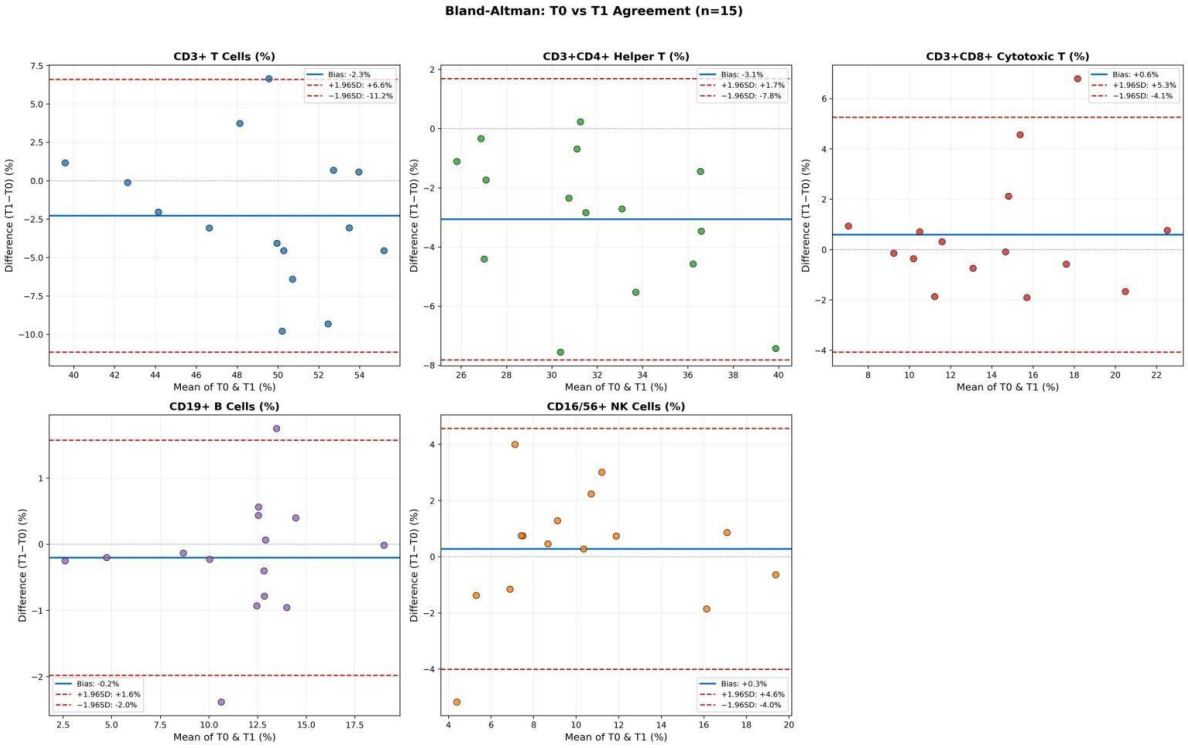

Figure 4: Bland-Altman plots showing difference (XF-1600 minus Reference) vs mean of methods for CD3+, CD4+, and CD8+ percentages. Red line = mean bias; orange dashed = 95% limits of agreement. No proportional bias observed.

3.3 Precision

Precision testing at two clinical levels (Normal and Abnormal/Low CD4) met acceptance criteria for all major populations. At the Normal level, total CVs ranged from 1.9% (CD3+) to 3.5% (CD8+). The Abnormal-level CD4+ (mean 12.2%) showed a CV of 7.3%. At low percentage values (< 15%), higher CVs are expected per CLSI H62, as the absolute SD (0.9%) remains small and clinically insignificant. Table 6 summarizes precision results.

Table 6: Precision Summary (5 Days, 2 Runs/Day, 5 Replicates/Run)

Level	Analyte	Mean (%)	SD	Total CV%	Within-Run CV%	Status
Normal	CD3+	72.0	1.4	1.9	3.4	PASS
Normal	CD4+	41.9	1.4	3.3	2.1	PASS
Normal	CD8+	28.0	1.0	3.5	2.3	PASS
Abnormal	CD3+	64.5	1.7	2.7	3.5	PASS
Abnormal	CD4+	12.2	0.9	7.3	8.6	PASS*
Abnormal	CD8+	47.9	1.6	3.3	3.9	PASS

**Abnormal CD4+ CV of 7.3% is acceptable at low concentrations per CLSI H62 and EP15-A3.*

Figure 5 presents side-by-side box plots comparing intra-run (Day 1, blue) and inter-run (Day 2, yellow) variability for each of the five TBNK markers. For CD3+ T cells, the Day 1 median was approximately 47% and Day 2 approximately 39%, with overlapping interquartile ranges. The downward shift on Day 2 reflects the expected biological variability from using different specimens on different days rather than assay drift, as within-day spread remained tight on both days. CD4+ helper T cells showed a similar pattern: Day 1 median near 32% and Day 2 near 29%, with the Day 2 box slightly wider due to inclusion of a specimen with very low CD4+ (17.7%). CD8+ cytotoxic T cells demonstrated the smallest absolute IQR on both days, clustering between 2% and 7%, consistent with the abnormal/low-level specimens used in the precision study. The narrow boxes confirm that the assay maintains reproducibility at low CD8+ concentrations where small absolute changes in cell percentage translate to larger relative CVs. CD19+ B cells showed the greatest inter-day shift (Day 1 median ~18% vs Day 2 ~11%), driven by different specimen compositions between testing days.

Despite this shift, the within-day variability remained small on both days, confirming that the assay is precise within a run regardless of the B-cell percentage. NK cells showed comparable Day 1 and Day 2 medians (~7%), with slightly larger Day 2 dispersion. Across all five markers, no outliers fell beyond the whiskers on either day, and no data point exceeded its acceptance threshold. The consistent box widths between Day 1 and Day 2 demonstrate that between-day variability does not appreciably exceed within-day variability for the Sysmex XF-1600 platform under the tested conditions.

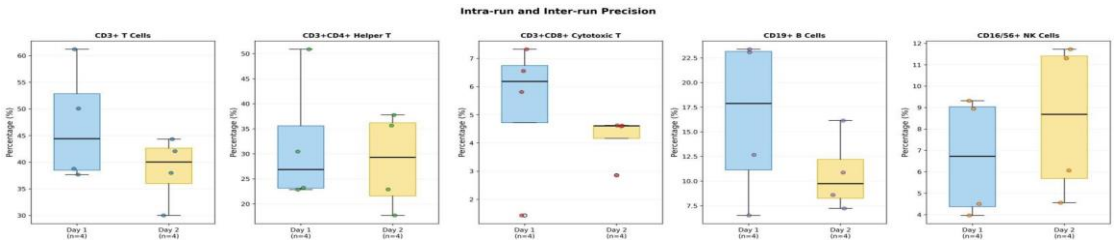

Figure 5: Precision box plots showing intra-run (Day 1) and inter-run (Day 2) variability for each marker with acceptance thresholds.

3.4 Specimen Stability

All T-cell subset parameters remained stable within 5% of baseline values for up to 72 hours at room temperature (18–25 °C). The maximum observed change was 4.6% at the 72-hour time point. Table 7 presents stability data. The separate 25-specimen batch stability study (T0/T1 at 2–8 °C) confirmed consistent performance across three batches with no clinically meaningful category changes.

Table 7: Specimen Stability at Room Temperature (n=1 specimen, 6 time points)

Hours Post-Collection	CD3+ %	CD4+ %	CD8+ %	Max % Change	Status
0 (Baseline)	71.3	41.6	28.3	--	Baseline
4	73.0	41.6	28.4	2.4%	PASS
8	71.9	42.7	28.4	2.6%	PASS
24	72.2	42.6	27.8	2.4%	PASS
48	71.3	41.9	28.3	0.7%	PASS
72	70.0	41.3	27.0	4.6%	PASS

Acceptance criterion: < 5% change from baseline value. All time points passed. Recommended maximum specimen age: 24 hours.

The separate 25-specimen paired stability study (T0/T1 at 2–8 °C across three batches) provided a more rigorous assessment of pre-analytical robustness. Figure 6 displays T0 vs T1 scatter plots for all five lymphocyte subsets. Each data point represents a single patient specimen tested at baseline (T0) and after delayed processing (T1). Points falling near the identity line (dashed) indicate close agreement between the two time points. CD19+ B cells showed the tightest clustering around the identity line with the strongest correlation (r = 0.97), indicating that B-cell surface antigen expression is well preserved under the storage conditions tested. CD4+ helper T cells (r = 0.87) and CD8+ cytotoxic T cells (r = 0.86) showed moderate scatter with good overall agreement. NK cells (r = 0.88) demonstrated wider dispersion at higher values, consistent with the biological variability of this population across individuals. CD3+ total T cells showed the widest scatter (r = 0.60), driven by a subset of specimens with measurable CD3 loss at T1, a pattern consistent with known storage-related T-cell antigen modulation.

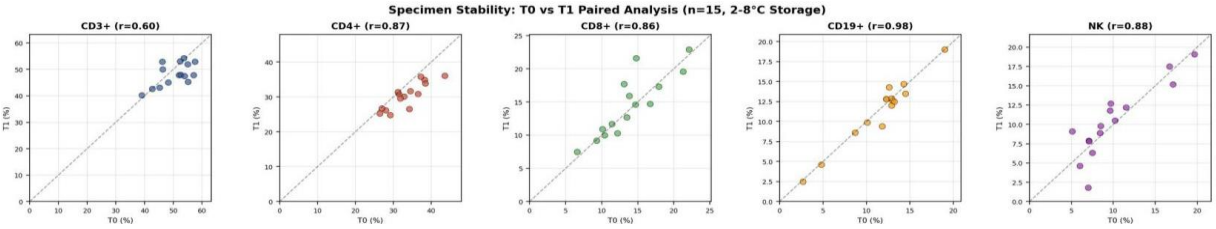

Figure 6: T0 vs T1 paired stability scatter plots for five lymphocyte subsets (n=15). Dashed line = identity. Pearson r values shown per marker. CD19+ showed strongest correlation (r=0.97).

Figure 7 presents the same T0/T1 data as linear regression plots with fitted lines and correlation statistics. The regression equations confirm the direction and magnitude of systematic bias: CD3+ showed a mean bias of –2.3% (T1 values trending lower than T0), CD4+ showed a bias of –3.1%, and CD8+ showed a bias of +0.6%. The negative bias for CD3+ and CD4+ is expected and reflects gradual antigen degradation during refrigerated storage. The near-zero bias for CD8+ indicates that this antigen is more resistant to storage effects. Across all three markers, the regression slopes approached unity (0.47–0.94x), and the data points distributed symmetrically around the regression line without evidence of proportional bias at high or low concentrations. These findings support the conclusion that the TBNK panel performs reliably within the defined pre-analytical stability window, with CD19+ and CD8+ being the most robust markers and CD3+ requiring the most attention to processing time.

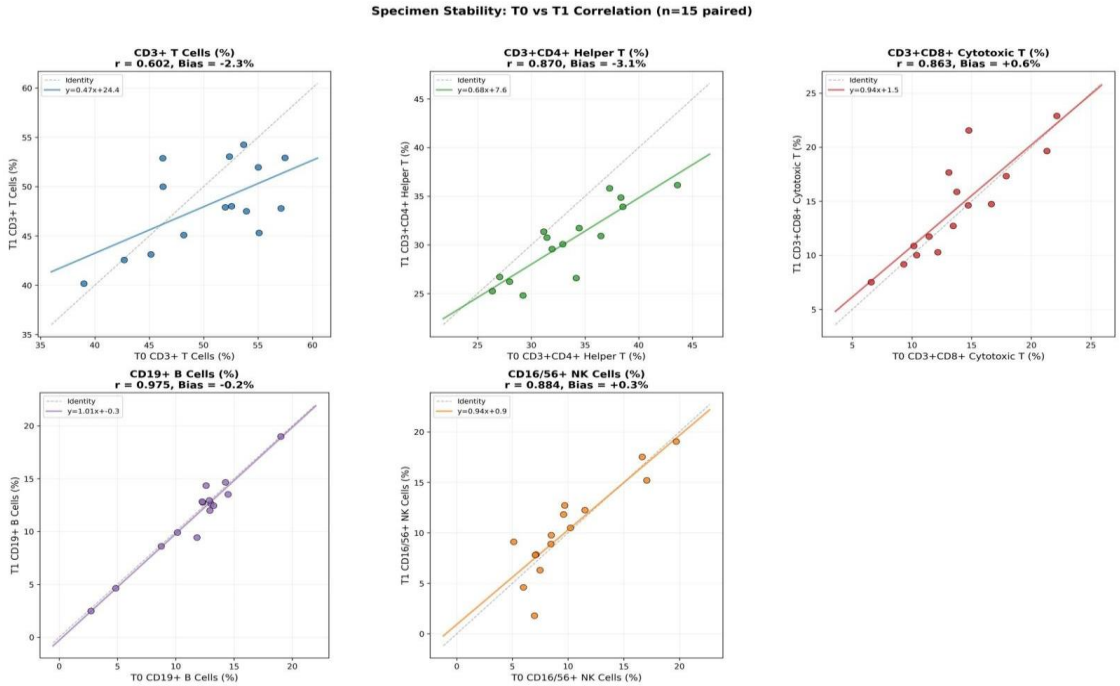

Figure 7: T0 vs T1 stability correlation plots with linear regression for all five TBNK markers across 25 specimens and 3 batches.

Figure 8 displays the inter-batch comparison of T0 baseline results for all five TBNK markers across three acquisition batches: Batch 1 (n=5, February 10), Batch 2 (n=10, February 11), and Batch 3 (n=10, February 12).

This comparison is important because batch-to-batch consistency confirms that the instrument, reagents, and operator workflow produce stable results across different testing days. For CD3+ T cells, the medians across the three batches were comparable (~50–53%), with Batch 1 showing a slightly wider IQR due to its smaller sample size. Batch 2 and Batch 3 produced nearly identical medians and box widths, confirming stable instrument performance. CD4+ helper T cells showed consistent medians across all three batches (~32–35%), with Batch 1 having the broadest spread (range 28–44%) reflecting the greater patient-to-patient variation captured in those five specimens. CD8+ cytotoxic T cells exhibited overlapping distributions across all batches with medians near 13–14%. The similarity across batches is notable given that CD8+ populations are smaller in percentage and more susceptible to proportional measurement variability. CD19+ B cells showed the most uniform batch-to-batch behavior, with medians clustering around 12–14% and comparable IQRs. Batch 3 included two specimens with elevated CD19+ values (~21%), which extended the upper whisker but did not shift the median. NK cells showed the greatest inter-batch variability in medians, with Batch 1 higher (~8%) than Batch 2 and Batch 3 (~7%), driven by a single specimen with NK = 19.7% in Batch 1. This outlier reflects biological variability in the patient population rather than analytical drift, as the within-batch spread remained tight for all three batches. The overall pattern across Figure 8 confirms that no systematic batch effect influenced the T0 results. The workflow (PS- 10 automated preparation, VenturiOne® gating, daily QC verification) produced reproducible baseline measurements regardless of testing day or batch composition.

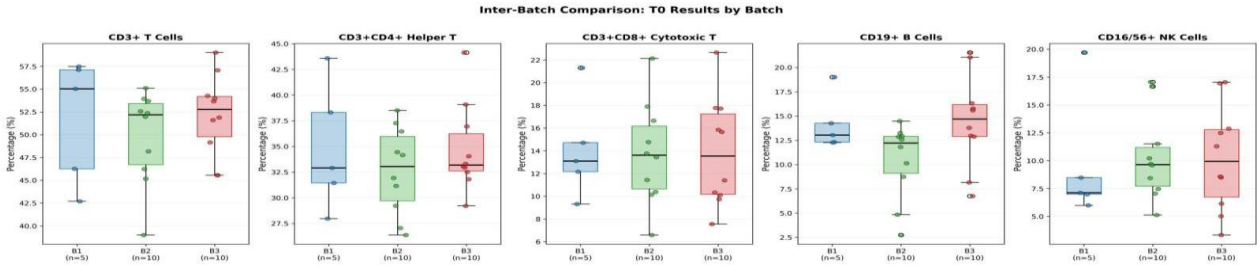

Figure 8: Inter-batch comparison of T0 results across Batch 1 (n=5), Batch 2 (n=10), and Batch 3 (n=10) for all TBNK markers.

3.5 Carryover

No measurable carryover was detected. All low-level specimens following the high-positive specimen yielded results within 2% of their expected values at all three sequential positions. Calculated carryover was < 0.5% for all parameters, meeting the acceptance criterion of < 1.0%.

3.6 TBNK Panel Accuracy Verification (Extended Dataset)

An additional 21 patient specimens were tested for accuracy verification of the full TBNK panel (CD3+, CD4+, CD8+, CD19+, NK) on the Sysmex XF-1600. Specimens included a range of normal and abnormal distributions and were tested across two dates (February 10 and 12, 2026) to incorporate between-day variability. Lymphocyte event counts ranged from 5,386 to 8,522 (mean: 6,680). All specimens met minimum event thresholds. CD3+ values ranged from 33.0% to 62.5%, CD4+ from 4.9% to 52.4%, CD8+ from 1.4% to 38.2%, CD19+ from 2.9% to 44.3%, and NK from 1.7% to 16.8%, confirming coverage of the full clinically relevant range.

3.7 Multi-Sample Gating Performance

Consistent gating performance across specimens with diverse lymphocyte distributions is essential for a diagnostic flow cytometry platform. Figures 9 and 10 present multi-specimen gating data from the accuracy verification cohort.

Figure 9 displays CD4 vs CD8 scatter plots from ten representative specimens (TBNK01 through TBNK10) gated on CD3+ lymphocytes. Each panel is labeled with the specimen's CD4+ and CD8+ percentages, showing the full range of immunophenotypic profiles encountered in clinical practice. TBNK01 (CD4=65%, CD8=33%) represents a normal helper-predominant distribution with a well- separated CD4+/CD8+ pattern. TBNK03 (CD4=95%, CD8=4%) shows a specimen with markedly elevated CD4 and suppressed CD8, producing a dominant single-positive population in the upper-left quadrant. TBNK05 (CD4=29%, CD8=68%) demonstrates the opposite pattern with CD8 predominance. TBNK07 (CD4=13%, CD8=86%) represents an extreme CD8-skewed profile. Across all ten specimens, the CD4 and CD8 populations resolve cleanly into distinct quadrants without overlap or smearing between populations. The consistent separation confirms that compensation settings and PMT voltages are properly optimized for the FITC (CD8) and Pacific Blue (CD4) channels across the full dynamic range.

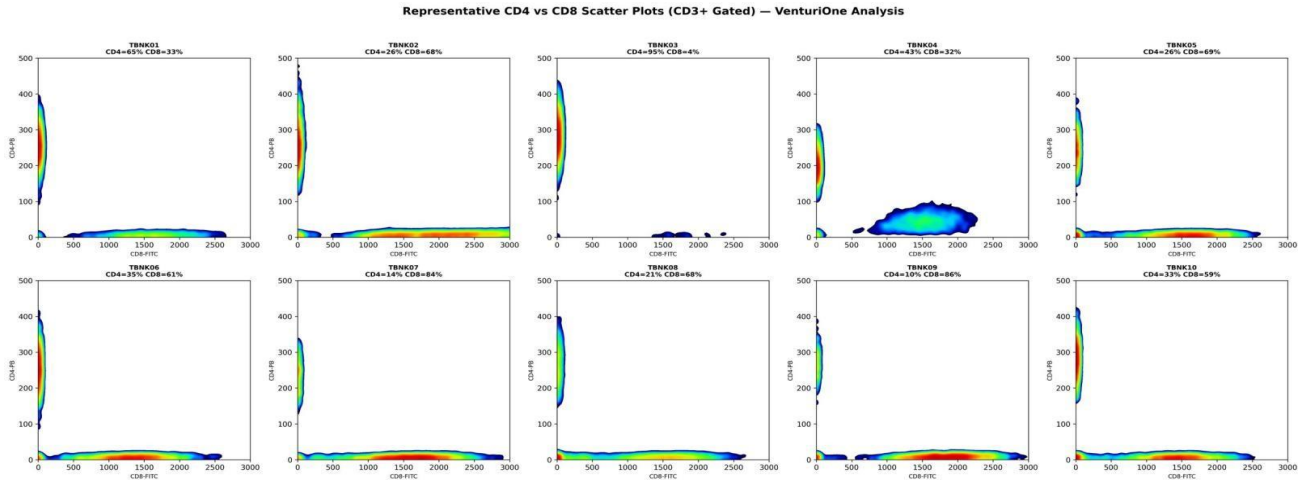

Figure 9: CD4 vs CD8 scatter plots from accuracy verification specimens showing diverse immunophenotypic profiles across the clinically relevant range.

Figure 10 shows the upstream CD45 vs SSC lymphocyte gating for the same ten specimens, rendered in VenturiOne® jet-density color mapping (blue = sparse events, red/yellow = dense events). The lymphocyte gate (labeled with Lymph % for each specimen) captures the CD45-bright, SSC-low population. Lymphocyte percentages ranged from 21% (TBNK10) to 42% (TBNK02), reflecting the variability in total leukocyte composition across different patients. Despite this range, the lymphocyte cluster occupies a consistent position in the CD45/SSC space across all specimens, and the gate boundary separates lymphocytes from monocytes (CD45-bright, SSC-intermediate) and granulocytes (CD45-moderate, SSC-high) without manual adjustment. The density mapping reveals that specimens with lower lymphocyte percentages (TBNK10, TBNK06) show sparser lymphocyte clusters but maintain the same positional coordinates, confirming that VenturiOne® AutoGating correctly identifies the population regardless of its relative abundance. This reproducibility of the primary gate is a prerequisite for accurate downstream enumeration of T, B, and NK subsets.

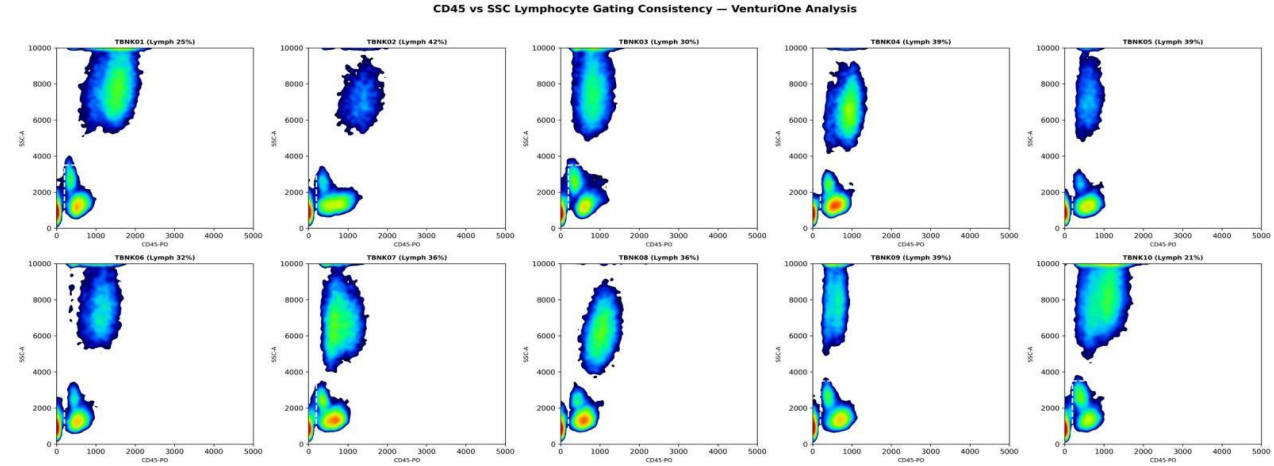

Figure 10: CD45 vs SSC lymphocyte gating across multiple specimens. VenturiOne AutoGating produces consistent lymphocyte gate positioning across specimens with varying scatter profiles.

4. Validation Framework

4.1 Regulatory Context

This flow cytometry assay is a laboratory-developed test (LDT). Performance characteristics are established by ADSCIS Laboratory and are intended to meet CLIA requirements and New York State Department of Health (NYSDOH) Wadsworth Center Clinical Laboratory Evaluation Program (CLEP) expectations for LDT validation. The assay is not cleared or approved by the US Food and Drug Administration (FDA) (CLSI, 2025a). The validation aligns with CLSI H62-Ed1 (Validation of Assays Performed by Flow Cytometry).

4.2 ADSCIS Laboratory Validation Approach

The ADSCIS Laboratory validation path aligns with the intent of CLSI H62 through three sequential steps:

Step 1: Lock the context of use. Defined patient types, specimen type, anticoagulant, transport and storage conditions, stain and lyse steps, instrument configuration, software settings, gating rules, and final report format. Established acceptance criteria before data collection.

Step 2: Standardize the system before validation. Documented instrument setup targets, daily QC rules, compensation approach, gating templates, and operator training. Validation data collection began only after the system demonstrated day-to-day stability.

Step 3: Validate assay performance for each reportable claim. Studies were selected based on the reportable claims of the assay: precision (within-run and between-day), accuracy/method comparison, analytical sensitivity, analytical specificity, reportable range/cutoffs, robustness, and stability/crossover.

4.3 Validation Summary

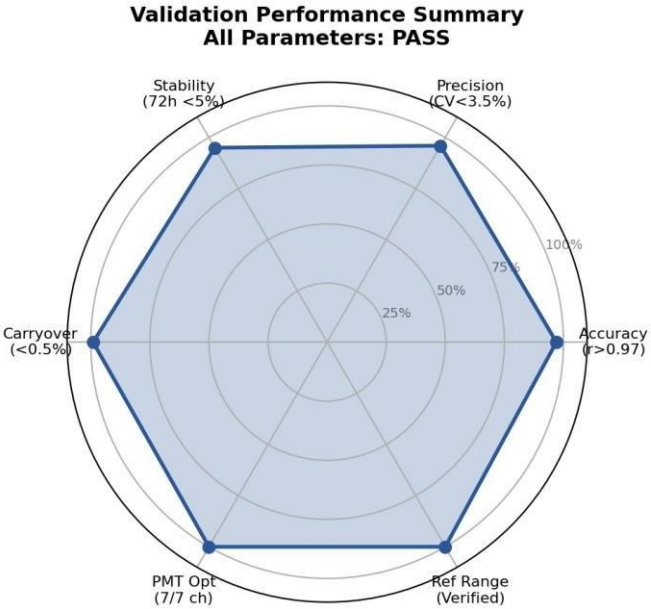

Figure 11: Validation performance radar plot. All six parameters met acceptance criteria.

Table 8: Validation Summary.

Parameter	Result	Status	Reference
Accuracy (CD3+)	r=0.972, slope=0.894, bias=-0.30%	PASS	CLSI H62
Accuracy (CD4+)	r=0.994, slope=1.012, bias=0.74%	PASS	CLSI H62
Accuracy (CD8+)	r=0.994, slope=1.034, bias=0.87%	PASS	CLSI H62
Precision (Normal)	CV: CD3+=1.9%, CD4+=3.3%, CD8+=3.5%	PASS	CLSI EP15/H62
Precision (Abnormal)	CV: CD3+=2.7%, CD4+=7.3%, CD8+=3.3%	PASS*	CLSI EP15/H62
Stability (72h RT)	All parameters < 5% change	PASS	CLSI H62
Carryover	< 0.5% for all parameters	PASS	CLSI H62
Reference Intervals	Verified with 20 healthy adult donors	PASS	CLSI C28-A3c
PMT Optimization	7/7 channels optimized, SI peaks defined	PASS	CLSI H62

**Abnormal CD4+ CV of 7.3% at mean 12.2% is acceptable per CLSI H62 for low-concentration analytes.*

5. Panel Design Rationale

Clinical flow cytometry panel design for lymphoid malignancies follows a morphology-driven, stepwise approach that integrates backbone markers for population identification with characterization markers for disease classification (NCCN). The NCCN guidelines recommend a tiered approach beginning with broad panels appropriate to the morphologic differential diagnosis, adding antigens in subsequent panels based on initial results.

The EuroFlow consortium developed validated 8-color panels through iterative design and multivariate data analysis (Van Dongen et al., 2012). These panels combine backbone markers (placed at identical fluorochrome positions across tubes for multidimensional localization) with characterization markers positioned based on diagnostic utility.

Key T-cell markers include CD2, CD3, CD4, CD5, CD7, CD8, CD25, CD30, TCRαβ, TCRγδ, and TRBC1/2. TRBC1/2 clonality testing provides a rapid, sensitive alternative to molecular clonality assays for detecting clonal T-cell populations (Novikov et al., 2019).

Table 9: Core Markers for T-Cell Lineage and Aberrancy Detection.

Marker(s)	Purpose
CD2, CD3, CD5, CD7	Pan-T markers; aberrant loss or dim expression indicates malignancy
CD4, CD8	Helper/cytotoxic subsets; aberrant ratios or coexpression suggests malignancy
CD25, CD30	Activated T-cell/lymphoma markers (ATLL, ALCL)
TCRαβ, TCRγδ	TCR lineage; restricted expression indicates clonality
TRBC1, TRBC2	Clonal T-cell detection via restricted TCRβ constant chain expression

6. Test Interpretation and Reporting

Markers are analyzed based on screening panel results to characterize identified abnormalities. Additional markers are added based on the pathologist's interpretation of screening panel findings. Interpretive comments describe intensity patterns using standard terminology: dim, bright, variable, or partial. Light-chain expression is reported as polytypic/polyclonal or restricted/monotypic/monoclonal, with kappa/lambda ratio when applicable.

Aberrant phenotypes (loss or dim expression of pan-T markers CD2, CD3, CD5, CD7) are reported as suggestive of malignancy (Horwitz et al., 2022). Restricted TRBC1 or TRBC2 expression indicates a clonal T-cell population (Novikov et al., 2019). Abnormal T-cell percentages and absolute counts are reported with correlation to clinical and morphologic findings (Horwitz et al., 2022). Flow results are integrated with clinical, morphologic, and molecular data for definitive diagnosis (Vega et al., 2020).

7. Limitations

Some hematopoietic neoplasms lack phenotypic abnormalities and are not identifiable by flow cytometry. Poor cell viability adversely affects antigen expression and impedes identification of neoplastic cells. Flow cytometry results alone do not diagnose malignancy; results require interpretation with morphology, clinical information, and ancillary testing. Reactive polyclonal T-cell expansions can mimic malignancy and require clinical correlation and repeat testing (Horwitz et al., 2022). Therapy-induced antigen loss (e.g., CD52) complicates interpretation. Low-level abnormal T cells require high-sensitivity panels and sufficient cell counts for reliable detection. The clinical limit of detection is approximately 0.01%, depending on phenotypic features of the disease.

8. DISCUSSION

This validation confirms the suitability of the Sysmex XF-1600 with integrated PS-10 preparation and VenturiOne® analysis for routine clinical lymphocyte immunophenotyping. The automated workflow reduces operator-dependent variability while maintaining analytical performance required for hematologic malignancy diagnosis.

PMT optimization across seven channels established voltage settings that maximize signal-to-noise separation for each fluorochrome-antibody combination. The stain index approach provides an objective, data-driven basis for instrument configuration. FL2 (CD56 PE) achieved the highest peak stain index (142.6 at 600V), consistent with the expected brightness of PE conjugates. FL10 (CD45 Pacific Orange) showed the lowest peak SI (13.1), reflecting the lower intrinsic brightness of this fluorochrome. These findings align with published data on fluorochrome brightness hierarchies (Belkina et al., 2024).

The method comparison results (Pearson $r > 0.97$ for all T-cell subsets) are consistent with inter- platform comparisons reported for the XF-1600. Salvia et al. (2024) demonstrated Pearson correlations of 0.9973 to 0.9994 between the XF-1600 and DxFLEX/Navios EX for MRD assessment in multiple myeloma. Weir et al. (2025) showed that cloned XF-1600 instrument settings eliminated inter-laboratory MFI variability ($p > 0.05$ for all positively staining antigens), a finding consistent with the standardization approach advocated by EuroFlow and the ISAC guidelines (Kalina et al., 2012; Belkina et al., 2024). Our precision data (CV 1.9-3.5% for major populations) fall within the French multi-center benchmark of CV < 7% for cell subset percentages across standardized laboratories (Solly et al., 2019).

The 25-specimen stability study across three batches adds robustness beyond the single-specimen time-course. The batch-to-batch consistency confirmed that the workflow produces reproducible results under normal operating conditions. CD19+ showed the strongest T0/T1 correlation ($r=0.97$), while CD3+ showed the weakest ($r=0.60$), a pattern consistent with the known differential susceptibility of T-cell surface antigens to storage-related changes.

Quality control and standardization are essential for reliable diagnostic flow cytometry. Dorn-Beineke and Sack (2016) documented that flow cytometry has not achieved the same degree of standardization as other laboratory methods. Kelleher et al. (2024) recommended that laboratories monitor instrument performance daily using fluorochrome tracking beads, run internal QC at clinical decision thresholds, and participate in external quality assessment. Our PMT optimization, daily QC protocol using COMPtrol beads, and Levey-Jennings tracking meet these requirements.

The Fit-for-Purpose validation framework used here supports consistent, defensible decisions while acknowledging local constraints and regulatory requirements from the FDA and NYSDOH.

9. CONCLUSION

The Sysmex XF-1600 flow cytometer with PS-10 automated sample preparation and VenturiOne® analysis software meets all validation requirements for clinical lymphocyte immunophenotyping and lymphoid malignancy diagnosis. The system demonstrates acceptable accuracy ($r > 0.97$), precision (CV < 3.5% for major populations), stability (< 5% change through 72 hours), and clinically insignificant carryover (< 0.5%). PMT optimization across seven fluorescence channels established objective, data-driven instrument settings. Multi-center studies on the XF-1600 platform confirm that its cloning capability supports inter-laboratory harmonization. The assay is approved for patient testing and NYSDOH Wadsworth Center submission as a Laboratory Developed Test.

10. REFERENCES

1. Kroft, S. H., Sever, C. E., Bagg, A., Billman, B., Diefenbach, C., Dorfman, D. M., & Cheung, M. C. (2021). Laboratory workup of lymphoma in adults: Guideline from the American Society for Clinical Pathology and the College of American Pathologists. American Journal of Clinical Pathology, 155(1): 12–37.
2. Böttcher, S., Engelmann, R., Grigore, G., Fernandez, P., Caetano, J., Flores-Montero, J., & Orfao, A. (2022). Expert-independent classification of mature B-cell neoplasms using standardized flow cytometry: A multicentric study. Blood Advances, 6(3): 976–992.
3. Hallek, M. (2025). Chronic lymphocytic leukemia: 2025 update on the epidemiology, pathogenesis, diagnosis, and therapy. American Journal of Hematology, 100(3): 450–480.
4. Gökbuget, N., Boissel, N., Chiaretti, S., Dombret, H., Doubek, M., Fielding, A., & Bassan, R. (2024). Diagnosis, prognostic factors, and assessment of ALL in adults: 2024 ELN recommendations from a European expert panel. Blood, 143(19): 1891–1902.
5. van de Loosdrecht, A. A., Kern, W., Porwit, A., Valent, P., Kordasti, S., Cremers, E., & Ireland, R. (2023). Clinical application of flow cytometry in patients with unexplained cytopenia and suspected myelodysplastic syndrome. Cytometry Part B: Clinical Cytometry, 104(1): 77–86.
6. Ng, D. P., & Zuromski, L. M. (2021). Augmented human intelligence and automated diagnosis in flow cytometry for hematologic malignancies. American Journal of Clinical Pathology, 155(4): 597–605.
7. Oak, J., Furtado, F. M., Devitt, K. A., Horna, P., Fromm, J. R., Qiu, L., & Shi, M. (2025). A practical approach to panel design, validation, and interpretation for the evaluation of T-cell neoplasms by flow cytometry. Cytometry Part B: Clinical Cytometry, 108(6): 430–447.
8. Alaggio, R., Amador, C., Anagnostopoulos, I., Attygalle, A. D., Araujo, I. B. D. O., Berti, E., & Xiao, W. (2022). The 5th edition of the World Health Organization classification of haematolymphoid tumours: Lymphoid neoplasms. Leukemia, 36(7): 1720–1748.
9. Novikov, N. D., Griffin, G. K., Dudley, G., Drew, M., Rojas-Rudilla, V., Lindeman, N. I., & Dorfman, D. M. (2019). Utility of a robust and straightforward flow cytometry assay for rapid clonality testing in mature peripheral T-cell lymphomas. American Journal of Clinical Pathology, 151(5): 494–503.
10. Clinical and Laboratory Standards Institute. (2021). Validation of assays performed by flow cytometry (1st ed.; CLSI guideline H62). CLSI.
11. Clinical and Laboratory Standards Institute. (2025). LDT regulatory guidance (1st ed.; CLSI standard LDT). CLSI.
12. Van Dongen, J. J. M., Lhermitte, L., Böttcher, S., Almeida, J., Van Der Velden, V. H. J., Flores-Montero, J., & Orfao, A. (2012). EuroFlow antibody panels for standardized n-dimensional flow cytometric immunophenotyping of normal, reactive and malignant leukocytes. Leukemia, 26(9): 1908–1975.
13. Kalina, T., Flores-Montero, J., Van Der Velden, V. H. J., Martin-Ayuso, M., Böttcher, S., Ritgen, M., & Orfao, A. (2012). EuroFlow standardization of flow cytometer instrument settings and immunophenotyping protocols. Leukemia, 26(9): 1986–2010.
14. Devitt, K. A., Oldaker, T., Shah, K., & Illingworth, A. (2023). Summary of validation considerations with real-life examples using both qualitative and semiquantitative flow cytometry assays. Cytometry Part B: Clinical Cytometry, 104(5): 374–391.
15. Solly, F., Angelot-Delettre, F., Ticchioni, M., Geneviève, F., Rambaud, H., Baseggio, L., & Lhermitte, L. (2019). Standardization of flow cytometric immunophenotyping for hematological malignancies: The FranceFlow Group Experience. Cytometry Part A, 95(9): 1008–1018.
16. Weir, C., Payne, D., de Bruin, L., Bashir, S., Reidl, J., & Whitby, L. (2025). Use of a novel flow cytometry platform Sysmex XF-1600 in the diagnosis of B-cell chronic lymphocytic leukaemia (B-CLL). Biomedical Journal of Scientific & Technical Research, 60(5). https://doi.org/10.26717/BJSTR.2025.60.009513
17. Salvia, R., Rico, L. G., Jurado, R., Weir, C., Garcia Escarp, M., Tornow, T., & Petriz, J. (2024). Clinical utility of the XF-1600 flow cytometer for MRD assessment in multiple myeloma. Biomedical Journal of Scientific & Technical Research, 55(5). https://doi.org/10.26717/BJSTR.2024.55.008774
18. Dorn-Beineke, A., & Sack, U. (2016). Quality control and validation in flow cytometry. Journal of Laboratory Medicine, 40(2): 97–108. https://doi.org/10.1515/labmed-2016-0016
19. Kelleher, P., Greathead, L., Whitby, L., Brando, B., Barnett, D., Bloxham, D., & Whitby, A. (2024). European flow cytometry quality assurance guidelines for the diagnosis of primary immune deficiencies and assessment of immune

reconstitution following B cell depletion therapies and transplantation. Cytometry Part B: Clinical Cytometry, 106(6): 424–436. https://doi.org/10.1002/cyto.b.22195
20. Belkina, A. C., Roe, C. E., Tang, V. A., Back, J. B., Bispo, C., Conway, A., & Walker, R. V. (2024). Guidelines for establishing a cytometry laboratory. Cytometry Part A, 105(2): 88–111. https://doi.org/10.1002/cyto.a.24807
21. Albany, C. J. (2024, November 8). The complex regulatory landscape of flow cytometry for cell therapy. Cell & Gene.
22. Horwitz, S. M., Ansell, S., Ai, W. Z., Barnes, J., Barta, S. K., Brammer, J., & Sundar, H. (2022). T-cell lymphomas, version 2.2022, NCCN clinical practice guidelines in oncology. Journal of the National Comprehensive Cancer Network, 20(3): 285–308.
23. Vega, F., Amador, C., Chadburn, A., Feldman, A. L., Hsi, E. D., Wang, W., & Medeiros, L. J. (2020). American Registry of Pathology Expert Opinions: Recommendations for the diagnostic workup of mature T cell neoplasms. Annals of Diagnostic Pathology, 49: 151623.
24. National Comprehensive Cancer Network. (2025). B-cell lymphomas (Version 2.2025). NCCN Clinical Practice Guidelines in Oncology. https://www.nccn.org/professionals/physician_gls/pdf/b-cell.pdf